The Impact of Ocean Surface Fluxes on a TOGA COARE Convective System

YANSEN WANG

Laboratory for Atmospheres, NASA/Goddard Space Flight Center, and Science Systems and Applications Inc., Greenbelt, Maryland

WEI-KUO TAO AND JOANNE SIMPSON

NASA/Goddard Space Flight Center, Greenbelt, Maryland

(Manuscript received 11 August 1995, in final form 11 June 1996)

ABSTRACT

A two-dimensional cloud-resolving model is linked with a TOGA COARE flux algorithm to examine the impact of the ocean surface fluxes on the development of a tropical squall line and its associated precipitation processes. The model results show that the 12-h total surface rainfall amount in the run excluding the surface fluxes is about 80% of that for the run including surface fluxes (domain-averaged rainfall, 3.4 mm). The model results also indicate that latent heat flux or evaporation from the ocean is the most influential factor among the three fluxes (latent heat, sensible heat, and momentum) for the development of the squall system. The average latent and sensible heat fluxes in the convective (disturbed) region are 60 and 11 W m^{-2} larger, respectively, than those of the nonconvective (clear) region due to the gust wind speed, a cool pool near the surface, and drier air from downdrafts associated with the convective activity. These results are in good agreement with observations.

In addition, sensitivity tests using a simple bulk aerodynamic approximation as well as a Blackadar-type surface flux formulation have predicted much larger latent and sensible heat fluxes than those obtained using the TOGA COARE flux algorithm. Consequently, much more surface rainfall was simulated using a simple aerodynamic approximation or a Blackadar-type surface flux formulation. The results presented here also suggest that a fine vertical resolution (at least in the lowest model grid point) is needed in order to study the interactive processes between the ocean and convection using a cloud-resolving model.

1. Introduction

It is well known that sensible heat, latent heat, and momentum fluxes between the ocean and the atmosphere are temporally and spatially complex in the region of active convection. Fresh water (precipitation) and cloud from atmospheric convection can alter the ocean surface processes by modifying the wind and temperature fields as well as the radiation budget on the ocean surface (Webster and Lukas 1992). The precipitation can also affect the salinity and the stratification of the ocean and hence the ocean wave spectrum, which is closely related to the atmosphere–ocean exchange. On the other hand, ocean surface processes can affect atmospheric convection by supplying additional heat and moisture. For example, Malkus (1958) and LeMone and Pennell (1976) demonstrated that the formation of oceanic cumulus clouds in the trade winds is controlled largely by marine boundary layer processes. Rotunno and Emanuel (1987) clearly showed that latent and sensible heat fluxes from the ocean are crucial for the development of tropical hurricanes. Tao et al. (1991) also indicated that sensible and latent heat fluxes can enhance surface precipitation and cloud coverage by 11% and 3%, respectively, compared with a simulation excluding the effects of ocean fluxes for a subtropical squall line.

In this study, a two-dimensional cloud-resolving model, the Goddard Cumulus Ensemble (GCE) Model, is linked with the TOGA COARE[1] bulk flux algorithm (Fairall et al. 1996) to quantify the effects of ocean surface fluxes, including the latent heat flux, the sensible heat flux, and the momentum flux, on the development of a tropical convective system. Sensitivity tests are also performed to assess various surface flux formulations (i.e., a bulk aerodynamic approximation

Corresponding author address: Dr. Y. Wang, Mesoscale Atmospheric Processes Branch, Code 912, NASA/GSFC, Greenbelt, MD 20771.
E-mail: wang@carmen.gsfc.nasa.gov

[1] The Tropical Ocean Global Atmosphere Coupled Ocean–Atmosphere Response Experiment (TOGA COARE) was conducted in the equatorial Pacific region during 1992–93. Its major objective was to gain a better understanding of the principal role of the western Pacific Ocean warm pool in oceanic and atmospheric (coupling) processes (Webster and Lucas 1992).

and a Blackadar surface flux formulation) and the vertical resolution used in the cloud-resolving model.

2. Model and model setup

The tool used in this study is the two-dimensional version of the GCE model. The model-simulated flow is assumed to be anelastically balanced; that is, sound waves have been filtered out by neglecting the local variation of air density with time in the mass equation. The cloud microphysics include a parameterized Kessler-type two-category liquid water scheme (cloud water and rain), and a parameterized Lin et al. (1983) or Rutledge and Hobbs (1984) three-category ice-phase scheme (cloud ice, snow, and hail/graupel). Shortwave (solar) and longwave (infrared) radiation parameterizations (Chou 1984, 1986) as well as a subgrid-scale turbulence (1.5-order) scheme are also included in the model.

The GCE model has recently implemented a multidimensional positive definite advection transport algorithm (MPDATA) (Smolarkiewicz 1983, 1984) with a nonoscillatory option (Smolarkiewicz and Grabowski 1990). All scalar variables (potential temperature, water vapor, turbulence coefficient, and all five hydrometeor classes) used forward time differencing and the MPDATA for advection. The MPDATA can advect only those variables that are either all positive or all negative. The dynamic variables, u, v, and w, can be positive or negative; therefore we used a second-order accurate advection scheme and a leapfrog time integration (kinetic energy semiconserving method). A stretched vertical coordinate (height increments from 40 to 1150 m) with 31 grid points was used to maximize resolution in the lowest levels of the model. A total of 1024 grid points was used in the horizontal with 750-m resolution. Details of the model can be found in Tao et al. (1993), Tao and Simpson (1993), and Simpson and Tao (1993).

a. Surface-layer parameterization

The surface flux parameterization used in this study is from the TOGA COARE flux algorithm (Fairall et al. 1996). This parameterization is primarily based on the bulk scheme developed by Liu et al. (1979), which has shown good agreement with observations (Bradley et al. 1991). The transfer coefficients for momentum, sensible heat, and latent heat fluxes are based on the Monin–Obukhov similarity theory of the atmospheric surface layer (Businger et al. 1971). This bulk scheme has been modified (Fairall et al. 1996; Bradley et al. 1991) to accommodate the very low surface wind situation.

According to the Monin–Obukhov similarity theory, the mean profiles of wind speed, potential temperature, and moisture have the following relations (Businger 1973):

$$\frac{U - U_s}{u_*} = \frac{1}{k_M}\left[\ln\left(\frac{z}{z_M}\right) - \Psi_M(\zeta)\right],$$

$$\frac{\theta - \theta_s}{\theta_*} = \frac{1}{k_H}\left[\ln\left(\frac{z}{z_H}\right) - \Psi_H(\zeta)\right],$$

$$\frac{q - q_s}{q_*} = \frac{1}{k_E}\left[\ln\left(\frac{z}{z_E}\right) - \Psi_E(\zeta)\right], \qquad (1)$$

where u_* is the friction velocity, θ_* is the temperature scaling parameter, and q_* is the moisture scaling parameter. Here, k_M, k_H, and k_E are the von Kármán constants, and z_M, z_H, and z_E are the roughness lengths. Here, Ψ_M, Ψ_H, and Ψ_E are the stability functions of ζ, which is equal to z/L (where L is the Monin–Obukhov length). The subscript s represents those variables at the ocean surface and the subscripts M, H, and E represent the parameters associated with momentum, sensible heat, and latent heat, respectively. The momentum, sensible heat, and latent heat fluxes can be expressed as

$$-\overline{u'w'} = C_M U^2 = u_*^2,$$

$$\overline{w'\theta'} = C_H U(\theta - \theta_s) = -u_*\theta_*,$$

$$\overline{w'q'} = C_E U(q - q_s) = -u_* q_*, \qquad (2)$$

where C_M, C_H, and C_E are the transfer coefficients for momentum, sensible heat, and latent heat. These bulk coefficients are related to the similarity profiles (1) as

$$C_M = \frac{k_M^2}{[\ln(z/z_M) - \Psi_M(\zeta)]^2}$$

$$C_H = \frac{C_M^{1/2} k_H}{[\ln(z/z_H) - \Psi_H(\zeta)]}$$

$$C_E = \frac{C_M^{1/2} k_E}{[\ln(z/z_E) - \Psi_E(\zeta)]}. \qquad (3)$$

The parameters, such as the roughness lengths, are closely related to the sea surface characteristics and the turbulence characteristics. In very low wind speed conditions, the similarity profile (1) becomes singular. This singularity was effectively eliminated by adding a convective velocity so that the ocean surface fluxes would not be zero under windless conditions (Bradley et al. 1991; Fairall et al. 1996).

The TOGA COARE bulk algorithm (surface-layer flux module) is called every 3 min[2] using the model-simulated wind, temperature, and moisture located at the lowest model grid level (20 m). The momentum, latent, and sensible heat fluxes derived from TOGA COARE bulk algorithm are then used for the cloud-

[2] Additional tests showed that surface precipitation differences between runs calling the flux algorithm every 7.5 s and every 180 s were small.

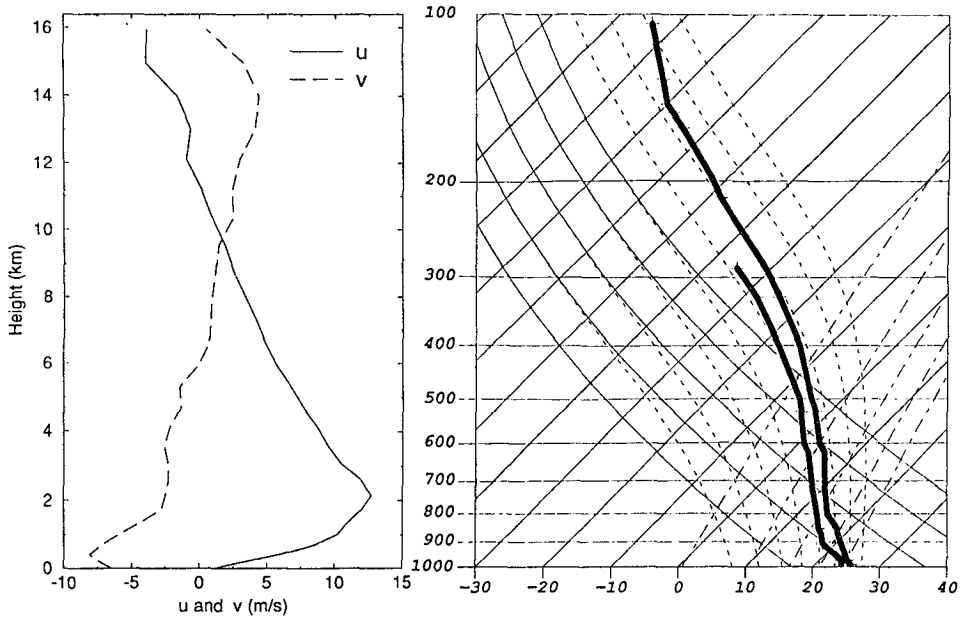

FIG. 1. The sounding used to initialize the model (kindly provided by M. LeMone).

resolving model. Observations (Bradley et al. 1991; Fairall et al. 1996; Young et al. 1992, 1995) indicated that the sea surface temperature (SST) is typically 1.0–1.5 K warmer than the surface layer air (including the "cool skin" effect). Observational data also indicated that the SST diurnal change is less than 0.2 K (Young et al. 1995; Lin 1995). Therefore, the SST was assumed to be a constant 28°C (about 1.2°C warmer than the initial air surface temperature). This SST is about the actual temperature used by Trier et al. (1996).

b. *TOGA COARE squall system*

A well-organized tropical oceanic squall system, observed during TOGA COARE on 22 February 1993 (Jorgensen et al. 1995; LeMone et al. 1995), was chosen to quantify the effect of ocean fluxes on the development and structure of the squall system. The GCE model was initialized with a sounding provided by Dr. LeMone (Fig. 1) and was integrated for 12 h. The corresponding CAPE[3] (convective available potential energy) and vertically integrated water vapor content for this squall line's environment were 1418 $m^2 s^{-2}$ and 6.049, respectively. Tropical oceanic convective systems are typically associated with a moderate CAPE and very moist environmental conditions. The convection is initialized in the model by a 2-km-deep cool pool (4.8 K of cooling over 10 min) in the middle of the computational domain.

TABLE 1. Model simulations in terms of surface flux options and vertical resolution.

	Flux algorithm	Vertical resolution (m)
Run 1	TOGA COARE	40
Run 1a	None	40
Run 1b	TOGA COARE No sensible heat flux	40
Run 1c	TOGA COARE No momentum flux	40
Run 1d	TOGA COARE No latent heat flux	40
Run 2a	Aerodynamic formula	40
Run 2b	Blackadar PBL fluxes	40
Run 3a	TOGA COARE	225
Run 3b	Aerodynamic formula	225

c. *Sensitivity tests*

Table 1 lists all of the sensitivity tests performed in this modeling study. Run 1 is the control run, which includes all three surface fluxes (latent heat, sensible heat, and momentum) computed from the TOGA COARE algorithm. In run 1a, all three surface-layer fluxes are neglected. The sensible heat flux, the momentum flux, and the latent heat flux are turned off,

[3] CAPE was calculated using GEMPAK, an atmospheric software package. A parcel averaged from the lowest 500 m of the atmosphere is lifted dry adiabatically to the LCL (lifted condensation level) then moist adiabatically thereafter. The CAPE is taken to be the sum, over all layers where the parcel temperature is warmer than the environment, of the parcel–environment temperature difference normalized by the environmental temperature and multiplied by gravity.

respectively, in runs 1b, 1c, and 1d. The impact of using different surface-layer modules on the squall system's development is also investigated. Runs 2a and 2b are the same as run 1 except for applying a bulk aerodynamic formula (AER) and a Blackadar surface flux module, respectively. Run 3a is the same as run 1 except that a 225-m vertical resolution at the lowest model grid is used. Temperature, vapor, and wind at 112.5 m instead of at 20 m are used to link the surface-layer module. Run 3b is the same as run 3a except that a bulk aerodynamic formula is used.

3. Results

a. Simulations with and without surface fluxes

Previous observations during GATE (Gaynor and Ropelewski 1979; Barnes and Garstang 1982) and TOGA COARE (Young et al. 1992; Bradley et al. 1991; Fairall et al. 1996) and from satellite retrievals (Chou et al. 1995) have demonstrated that deep convection can greatly influence ocean surface fluxes. By linking the GCE model with the TOGA COARE bulk surface-layer flux module, we can study the interaction between the ocean surface and atmospheric convection. The surface fluxes (Figs. 2a–c) varied significantly in the horizontal in the presence of the convection, with very large fluxes occurring at the leading edge of the squall line. This phenomenon can be explained by examining the spatial structures of the wind, moisture, and temperature fields. First, the wind field at the first model vertical layer (20 m) (Fig. 2e) had a maximum (or gust front) located at the leading edge of the cloud system. This maximum wind speed increased the fluxes. Second, the development of a cool pool (Fig. 2d) enhanced the temperature difference between the ocean surface and the atmosphere, and therefore also increased the sensible and latent heat fluxes. And third, the rear inflow into the squall line brought down drier air from the midtroposphere and increased the moisture deficit (Fig. 2f) in the surface layer and therefore enhanced the latent heat flux.

The modeled convective system was sampled at three different times (4, 6, and 8 h) to identify the most important variable for increasing fluxes between the ocean surface and the atmosphere. Table 2 lists correlation coefficients associated with wind speed, potential temperature, and moisture in the latent heat fluxes, sensible heat fluxes, and friction velocity. As expected, the momentum flux is highly correlated (0.93 correlation coefficient) to the wind speed. On the other hand, the model results indicate that the latent and sensible heat fluxes are more closely correlated to the temperature and water vapor (moisture) difference (0.82–0.94), than to the wind speed (0.68–0.70). These results suggest that the heat fluxes are largely driven by the temperature and moisture differences between the sea surface and the atmosphere, while the wind speed is less influential except at the leading edge of the convection. However, under weak wind conditions, Jabouille et al. (1994) suggested that the variation of heat flux is largely controlled by wind speed. Young et al. (1995) also pointed out that the increase in air–sea temperature difference and the increase in wind speed due to convection are the major causes for the increase in sensible and latent heat fluxes. The relative importance of wind or thermodynamic contrast is both a function of parameter space and timescale.

Table 3 shows the accumulated 12-h rainfall normalized by the model domain grid number (1024). The model simulation without surface fluxes (run 1a) produces only 82% of the rainfall compared to that from the simulation including surface fluxes (run 1). The precipitation rates with and without surface fluxes are rather similar during the first 5–6 h of the simulation. Afterward, the results from the two runs diverge rather quickly (see Fig. 3). To compare the cloud characteristics and wind circulations in the simulations with and without surface fluxes, the total hydrometer fields (sum of rain, cloud water, cloud ice, snow, and graupel) after 10 h of integration time are shown in Fig. 4 and the corresponding streamlines in Fig. 5. The total hydrometer content is substantially greater and cloud coverage is larger in the run with surface fluxes compared to that without surface fluxes. The wind circulation, both updraft and downdraft, is stronger for the run with surface fluxes. This is due to the fact that the moisture and heat supplied by the surface fluxes maintain a quasi-steady CAPE in the simulation domain. On the other hand, the CAPE significantly decreased (from 1418 to 980 J kg^{-1}) in the run without surface fluxes. This unrealistic decrease in CAPE is caused by convection-induced subsidence, which brought drier air to the lower troposphere. These results clearly indicate that ocean surface fluxes can play a significant role in tropical convection. However, shallow convection along the leading edge of the simulated system as well as the dominance by warm rain processes are characteristics still present in both runs. Secondary updraft development 10–20 km away from the leading edge of the system are also simulated in both runs. This feature is also found in the radar observations (Jorgensen et al. 1995; LeMone et al. 1995). (A paper including 3D model results will be forthcoming and will discuss these features in more detail.)

To assess the sensitivity of convective activity to latent heat flux, sensible heat flux, and momentum flux individually, three different runs were made: run 1b (no sensible heat flux), run 1c (no momentum flux), and run 1d (no latent heat flux). The results indicated that the surface latent heat flux had the most influence, while the surface sensible heat flux had the least influence on surface precipitation processes (Table 3). This is because the Bowen ratio (ratio of sensible heat to latent heat) is small, usually about 0.15–0.2 in both the active convective region as well as the nonconvective

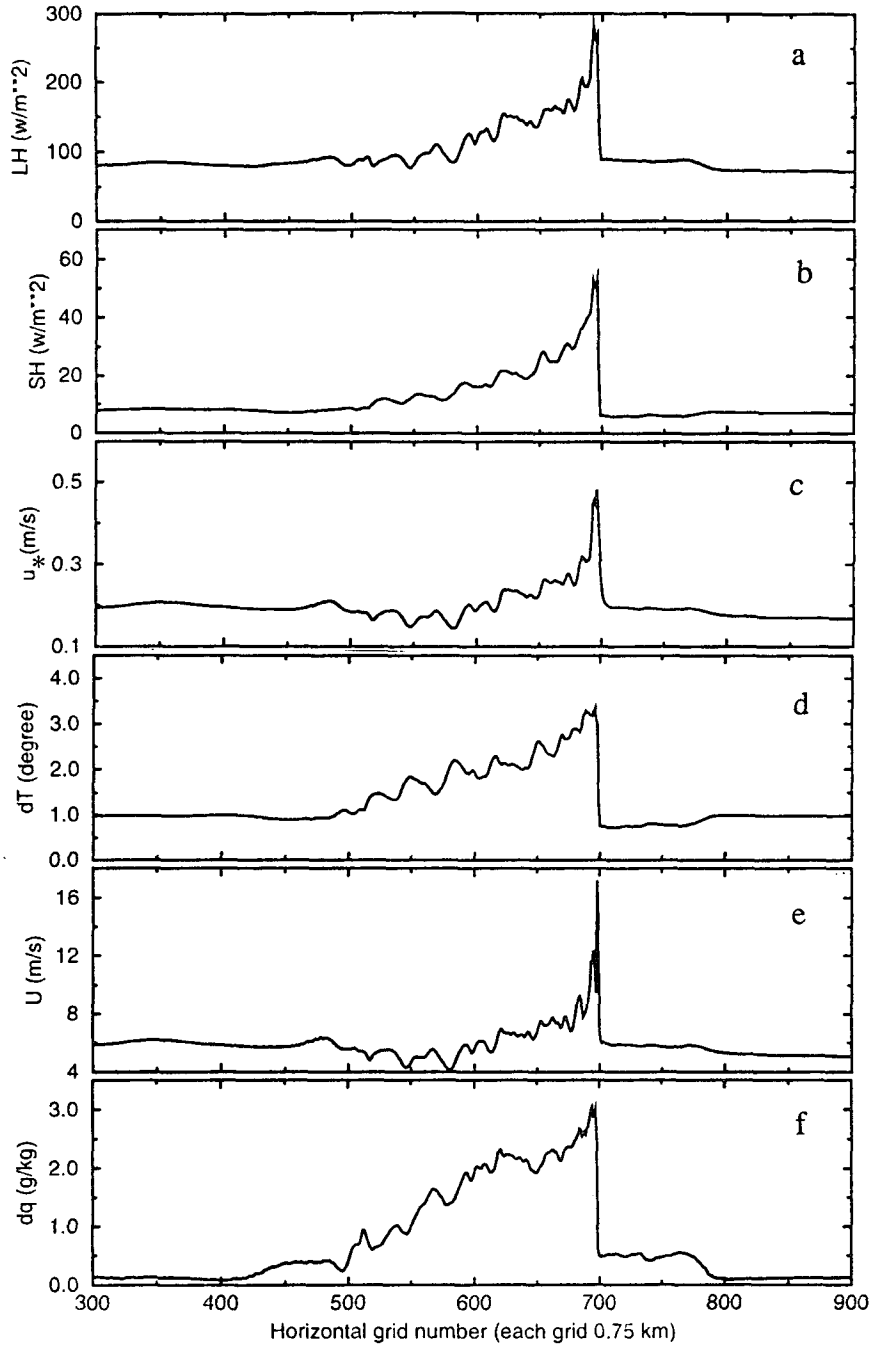

FIG. 2. Spatial variation of (a) latent heat flux (LH), (b) sensible heat flux (SH), (c) friction velocity (u_*), (d) temperature difference between sea surface and at 20 m (dT), and (f) vapor mixing ratio difference between sea surface and at 20 m (dq). These plots are taken from the simulated results at 6 h.

region (also see Table 4). As expected, the role of momentum flux is to suppress convective activity by reducing the wind speed in the surface layer and consequently the latent and sensible heat flux. Indeed, the run without surface momentum flux produced more rainfall. This suppression of heat and moisture fluxes due to momentum flux lowering of the surface wind speed is more important in the undisturbed region since the wind speed is already fairly low (around 5 m s^{-1}) and the transfer coefficients C_H and C_E as a result are

TABLE 2. Correlation coefficient matrix (each surface flux is correlated with wind speed, air–sea temperature difference, and air–sea vapor mixing ratio difference).

	Latent heat flux (W m^{-2})	Sensible heat flux (W m^{-2})	Friction velocity u_* (m s^{-1})
U (m s^{-1})	0.68	0.70	0.93
D_T (K)	0.89	0.94	0.57
Dq (g kg^{-1})	0.87	0.82	0.50

U: wind speed at 20 m.
D_T = SST − T (at 20 m).
Dq = q_s (at SST) − q (at 20 m).

TABLE 3. Domain-averaged surface rainfall amounts and percentage of rainfall compared with the control run (run 1).

	Domain averaged rainfall (mm)
Run 1 (COARE)	3.4 (100%)
Run 1a (no all fluxes)	2.8 (82%)
Run 1b (no S-H-F)	3.3 (97%)
Run 1c (no M-F)	3.7 (109%)
Run 1d (no L-H-F)	2.7 (79%)

more sensitive to the wind speed (Liu et al. 1979). Also, in the wind condition, a small change of 1 m s^{-1} means a large percentage change of wind, hence a large percentage change of fluxes.

b. *Sensitivity tests using other surface-layer flux modules*

The TOGA COARE bulk flux algorithm was developed and calibrated with the TOGA COARE surface flux dataset. It gives results that agree very well with other turbulence-based techniques, such as the eddy correlation method (Bradley et al. 1991) and the inertial dissipation method (Fairall and Larson 1986). Simple bulk aerodynamic methods (hereafter AER), such as those by Malkus (1962) and Roll (1965), have been used frequently in cloud-resolving models as well as in hurricane models. In the AER formulation, the drag coefficient for momentum and heat (both sensible and latent) is expressed as a function of wind speed:

$$C_d = 10^{-3}(1.1 + 0.04U), \qquad (4)$$

where U is the wind speed in meters per second. The major difference between TOGA COARE and AER is that the drag coefficient depends only on the wind speed in the AER formulation, whereas the drag coefficient depends on both dynamic and thermal stability functions through the Monin–Obukhov similarity theory in the TOGA COARE flux algorithm (see section 2a). Another surface flux formulation is based on the Blackadar PBL (BLK hereafter), which has been widely applied in modeling studies associated with midlatitude continental convective systems (Zhang and Anthes 1982). The surface layer is classified as either stable, mechanically driven turbulence, forced convection, or free convection based on the bulk Richardson number. The Monin–Obukhov similarity theory is used to parameterize the surface fluxes for each stability condition. In unstable conditions, there is a convective velocity that is proportional to the temperature difference between the surface and the first model layer and is used to parameterize the convective scaling velocity in the mixed layer.

The exchange coefficients in the AER method and in the TOGA COARE flux algorithm are mainly different in two ways. First, in the lower wind speed region (<4 m s^{-1}), the exchange coefficients in the TOGA COARE flux algorithm increase with decreasing wind speed in order to account for the convective exchange at low wind speeds. Second, the coefficients in the AER method linearly increase with respect to the wind speed, while the C_E and C_H in the TOGA COARE algorithm go down with wind speed when wind speed is greater than 5 m s^{-1} (see Fairall et al. 1996). These differences in the exchange coefficients probably reflect the differences in the datasets on which the algorithms were based. For example, a review on this subject (Garratt 1977) revealed a substantial midlatitude bias in the field measurements with most of the data obtained in the 4–15 m s^{-1} range. The TOGA COARE flux algorithm (Fairall et al. 1996) was specifically based on the data from TOGA COARE. It has advantages over the other flux schemes as will be shown in a later part of this note.

Table 4 lists the accumulated domain-normalized surface rainfall amounts as well as the horizontally averaged latent and sensible heat fluxes for the disturbed (convective) and undisturbed (cloud-free) areas sim-

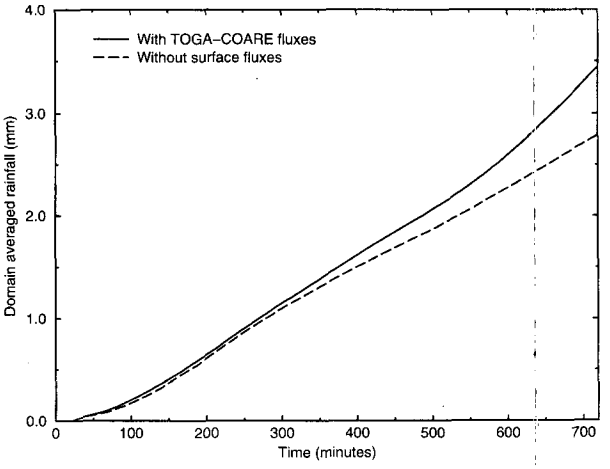

FIG. 3. Domain-averaged rainfall simulated with TOGA COARE fluxes and without fluxes.

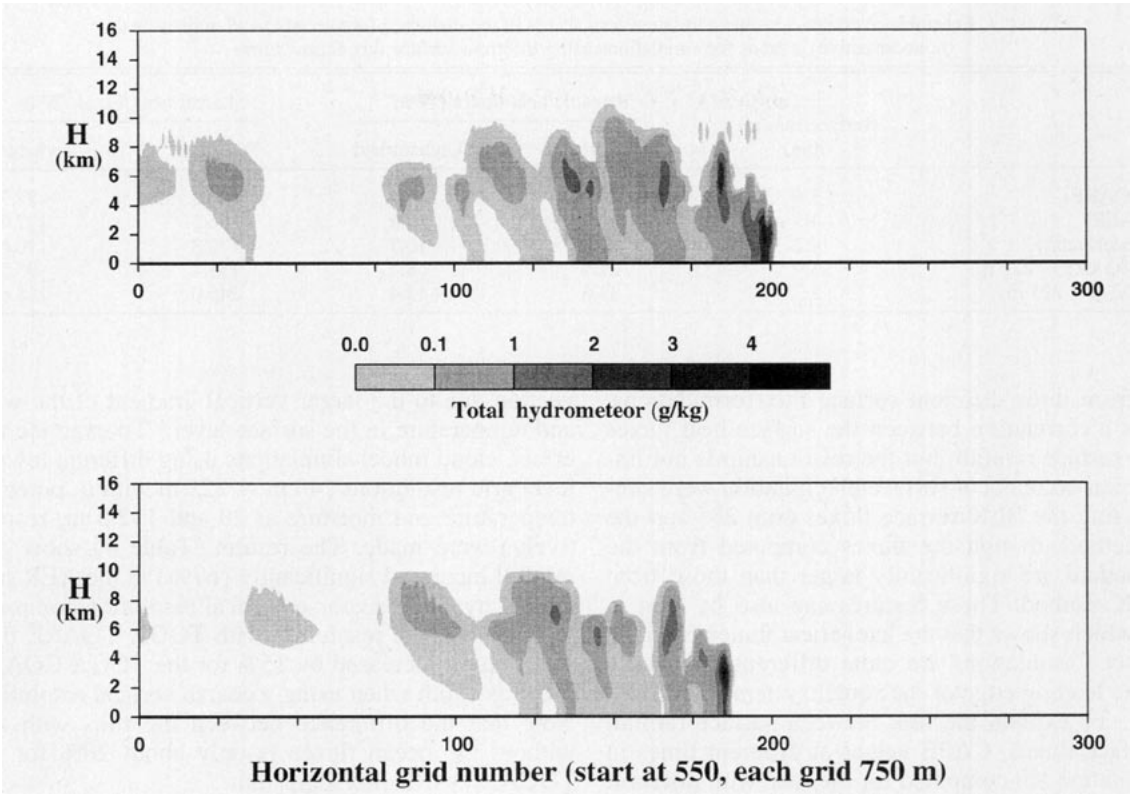

FIG. 4. Total hydrometeor content (sum of rain, cloud water, cloud ice, snow, and graupel) at 10 h into the simulation.

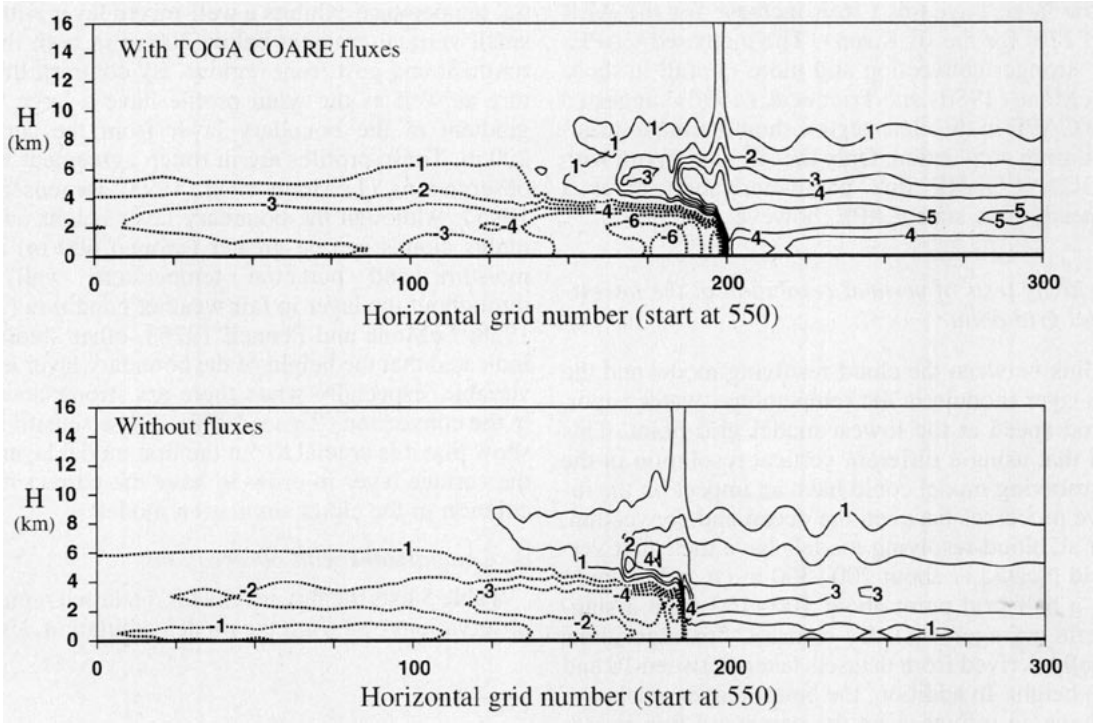

FIG. 5. Mass streamfunction ($\times 10^4$ g cm^{-1} s^{-1}) at 10 h into the simulation.

TABLE 4. Ensemble-averaged sensible and latent heat fluxes in the disturbed (convective) and undisturbed (nonconvective) regions for simulations using different surface flux formulations.

	Surface rainfall (mm)	Sensible heat fluxes (W m^{-2})		Latent heat fluxes (W m^{-2})	
		Disturbed	Undisturbed	Disturbed	Undisturbed
Run 1 (COARE)	3.4	20.9	8.4	142.2	81.7
Run 2a (AER)	4.5	31.1	12.9	206.5	127.7
Run 2b (Blackadar)	4.2	24.4	10.7	170.8	110.6
Run 3a (COARE—225 m)	3.9	21.9	8.4	155.4	95.2
Run 3b (AER—225 m)	5.7	33.6	13.4	245.0	158.6

ulated from three different surface flux formulations. There is a correlation between the surface heat fluxes and the surface rainfall, but the relationship is not linear. Similar amounts of surface precipitation were simulated using the BLK surface fluxes (run 2b) and the AER method, though the fluxes computed from the AER method are significantly larger than those from the BLK method. These features can also be seen in Fig. 6, which shows that the latent heat fluxes from the three flux formulations are quite different, especially along the leading edge of the squall system (gust front region). To explain the link between surface rainfall and surface fluxes, CAPE values at different times in the simulation are computed for the runs with different flux formulation. CAPE values did not vary much over the course of the simulation using the TOGA COARE fluxes (1418 J kg^{-1} at the beginning and 1492 J kg^{-1} at the end of simulation, 5% increase). However, CAPEs in the runs using AER and BLK formulations did show large increases (16% increase for the AER run and 17% for the BLK run). The increased CAPEs caused stronger convection and more rainfall in those runs. LeMone (1980) and Trier et al. (1996) suggested that the CAPE in the clear region should remain quasi-steady during convection. Only the simulation run with the TOGA COARE flux parameterization gives a quasi-steady base state CAPE, however.

c. *Sensitivity tests of vertical resolution at the lowest model grid point*

The link between the cloud-resolving model and the surface-layer module is the temperature, water vapor, and wind speed at the lowest model grid point. This implies that using a different vertical resolution in the cloud-resolving model could have an impact on the interactive processes between the ocean and convection. Almost all cloud-resolving models have their first vertical grid located at about 200–300 m (u and v would start at a half grid point about 100–150 m in a staggered grid arrangement). By contrast, flux algorithms are usually derived from datasets taken between 10 and 20 m in height. In addition, the bottom layer resolution might have an influence on the computed flux values and therefore affect the overall development of the convection due to the larger vertical gradient of the wind and temperature in the surface layer.[4] To examine this effect, cloud model simulations using different lowest-level grid resolutions (40 m vs 225 m with u, potential temperature and moisture at 20 and 112.5 m, respectively) were made. The results (Table 4) show that rainfall increased significantly (67%) in the AER runs simply by using a coarse vertical resolution compared to a fine vertical resolution with TOGA COARE flux. The rainfall increased by 15% for the TOGA COARE flux algorithm when using a coarse vertical resolution. Note that the difference between the runs with and without the ocean fluxes is only about 20% for the TOGA COARE flux algorithm.

The coarse vertical resolution (225 m) significantly overestimated the surface fluxes, especially in the disturbed region (Table 4). These results can perhaps be explained by the wind, potential temperature, and moisture profiles in the boundary layer (Fig. 7). The potential temperature exhibits a well-mixed layer with a very small vertical gradient below 200 m in both the environment and gust front regions. By contrast, the moisture as well as the wind profile have a large vertical gradient in the boundary layer from the surface to 200 m. These profiles are in rough agreement with the observations (LeMone et al. 1995; Jorgensen et al. 1995). Although the boundary layer height under cumulus clouds can be greater (around 600 m) and the moisture and potential temperature well mixed throughout the layer in fair weather condition (Malkus 1958; LeMone and Pennell 1976), other studies have indicated that the height of the boundary layer is highly variable, especially when there are strong downdrafts in the convection (Zipser 1977). These sensitivity tests show that it is crucial to put the first model layer within the surface layer in order to have the correct flux calculation in the cloud simulation model.

d. *Comparisons with observations*

Table 5 lists the flux results for disturbed region from observations and from the model simulation. Using the

[4] The modeled temperature and water vapor profiles agree fairly well with measurements presented by LeMone et al. (1995).

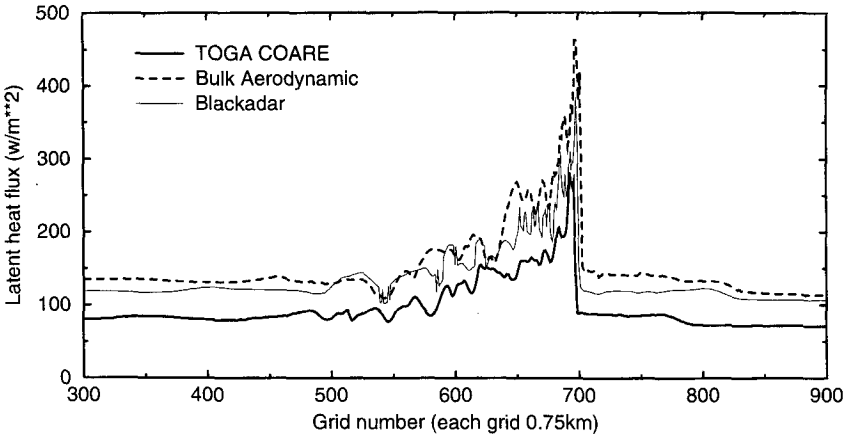

FIG. 6. Latent heat fluxes simulated from different surface flux formulations at 6 h.

TOGA COARE flux algorithm, LeMone et al. (1995) have computed sensible and latent heat fluxes from aircraft measurements at a height of 158 m. To make a valid comparison, we have also computed the fluxes using the model-generated wind, temperature, and moisture at 156 m (second model grid height). These results agree well with the observations. In addition, the flux values computed using model data at the 20-m level also compared favorably with those measured at 10 m during a pilot cruise observation (Young et al. 1992). Young et al. (1995) also reported on a very extensive set of flux observations from the TOGA COARE intensive observation period. The results showed great similarity in the convective wake characteristics between individual wakes and in the composite time series, despite the observations coming from different locations and seasons. Our flux calculations using the TOGA COARE algorithm and the cloud model predicted variables give slightly higher values in the convective region, probably due to the stronger than average convection in this squall-line case. The relative increases in flux in our simulation due to the convective wake are 248%, 170%, and 200% for sensible heat, latent heat, and momentum, respectively. Those values agree fairly well with the percentage increases reported by Young et al. (1995).

Good agreement in surface fluxes may imply that the modeled wind, temperature, and moisture fields in the lower troposphere are realistic. For example, we found that the simulated cooling and maximum wind speed near the leading edge of the convective system (Fig. 2) agreed well with the observations. For the same TOGA COARE case, Jorgensen et al. (1995) reported a 15 m s^{-1} wind speed at the leading edge of the convective line. Our simulation gives similar results. The wind speed is 16 m s^{-1}, the cooling is 3.8 K, and the drying is 3 g kg^{-1} at the leading edge of the convective line. However, the model simulation did not produce the strong wind observed further back from the leading edge. It is probably due to three-dimensional effects, which the two-dimensional model is unable to simulate. For a different TOGA COARE case, Parsons et al.

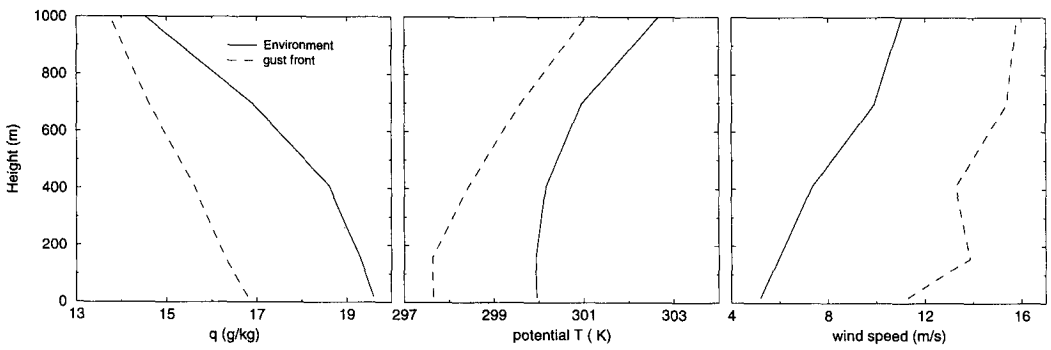

FIG. 7. Boundary layer profiles at the gust front and in the clear area at 6 h.

TABLE 5. Comparison of the sensible and latent heat fluxes simulated with the TOGA COARE flux algorithm and from observations.

	Sensible heat fluxes (W m^{-2})		Latent heat fluxes (W m^{-2})	
	Disturbed	Undisturbed	Disturbed	Undisturbed
LeMone et al. (1995) (158 m)	34	NA	192	NA
Run 1 (156 m)	32.5	11.0	189.7	108.3
Run 1 (20 m)	20.9	8.4	142.2	81.7
Young et al. (1992) (10 m)	14.4	7.7	122.3	101.1

(1994) reported a 4.5°C cooling, a 10–12 m s^{-1} wind speed, and a 2 g kg^{-1} drying at the leading edge of the convection.

4. Summary and conclusions

A two-dimensional cloud-resolving model is linked with a TOGA COARE flux algorithm to examine the impact of ocean surface fluxes on tropical squall line (a strong convective system) development and the associated precipitation processes. The simulated total surface rainfall amount in the run without surface fluxes is about 80% of the rainfall simulated with surface fluxes. The results indicate that surface fluxes can have a significant influence on the squall structure and the intensity of the circulation within the squall system. Sensitivity tests indicated that latent heat (moisture) flux is the most influential factor among the three fluxes (latent heat, sensible heat, and momentum) for the squall system's development. The simulation results also indicate that the heat and momentum fluxes in the convective region can be significantly increased due to increases of wind and thermodynamic contrast in the atmospheric surface layer in the convective region. These results are in agreement with many observational studies (Barnes and Garstang 1982; LeMone et al. 1995; Bradley et al. 1991; Young et al. 1992; Fairall et al. 1996; Young et al. 1995).

Since a large vertical wind and moisture gradient existed in the marine boundary layer, the lowest model grid point had to be placed close to the surface in order to compute the surface fluxes correctly. The model results show that a fine vertical resolution (at least in the lowest model grid point) is needed to study the impact of surface fluxes on oceanic precipitation events using a cloud-resolving model. Sensitivity tests using an aerodynamic approximation as well as a Blackadar surface flux formulation predicted larger latent and sensible heat fluxes than those from the TOGA COARE flux algorithm. These differences can cause large deviations in the amount of precipitation simulated. A large database gives the TOGA COARE flux algorithm an advantage in the simulation of tropical convective systems.

The use of a two-dimensional model may limit our ability in modeling the cloud system, because convective dynamics are inherently three-dimensional. Squall systems, however, are more or less two-dimensional when compared with supercell types of convection (e.g., Rotunno et al. 1988; Barnes and Sieckman 1984; Houze 1989). Recent three-dimensional GCE model results for a TOGA COARE squall system have shown that the two-dimensional results are still valid in that surface fluxes can enhance the precipitation processes. The overall structure did show some differences along the edges of the squall system between runs with and without radiation, however. We will report the three-dimensional results in the near future.

Acknowledgments. The authors thank Dr. M. LeMone for providing the TOGA COARE sounding. The authors also thank Drs. M. LeMone and E. Zipser for discussing the initial conditions used for model simulation. Mr. S. Lang and Dr. J. Halverson read the manuscript and provided many useful suggestions. We also thank Dr. M. LeMone and two anonymous reviewers for their constructive comments that improved the clarity of the presentation in this paper.

This work is supported by the NASA Headquarters Radiation, Dynamics and Hydrology Branch under Contract 460-23-54 and by the NASA TRMM Project under Contract 461-57-22. These authors are grateful to Drs. J. Theon and R. Kakar for their support of this research. Acknowledgment is also made to NASA/Goddard Space Flight Center for computer time used in the research.

REFERENCES

Barnes, G. M., and M. Garstang, 1982: Subcloud layer energitics of precipitating convection. *Mon. Wea. Rev.*, **110,** 102–117.

——, and K. Sieckman, 1984: The environment of fast- and slow-moving tropical mesoscale convective cloud lines. *Mon. Wea. Rev.*, **112,** 1782–1794.

Bradley, E. F., P. A. Coppin, and J. S. Godfrey, 1991: Measurements of sensible and latent heat flux in the western tropical Pacific Ocean. *J. Geophys. Res.*, **96,** 3375–3389.

Businger, J. A., 1973: Turbulent transfers in the atmospheric turbulence. *Workshop on Micrometeorology,* Boston, MA, Amer. Meteor. Soc., 67–100.

——, J. C. Wyngaard, Y. Izumi, and E. F. Bradley, 1971: Flux profile relationships in the atmospheric surface layer. *J. Atmos. Sci.*, **28,** 181–189.

Chou, M.-D., 1984: Broadband water vapor transmission functions for atmospheric IR flux computation. *J. Atmos. Sci.*, **41,** 1775–1778.

——, 1986: Atmospheric solar heating rate in the water vapor bands. *J. Climate Appl. Meteor.*, **25,** 1532–1542.

Chou, S.-H., R. M. Atlas, C.-L. Shie, and J. Ardizzone, 1995: Estimates of surface humidity and latent heat fluxes over oceans from SSM/I data. *Mon. Wea. Rev.,* **123,** 2405–2425.

Fairall, C. W., and S. E. Larsen, 1986: Inertial-dissipation methods and turbulent fluxes at the air–ocean interface. *Bound.-Layer Meteor.,* **34,** 287–301.

——, E. F. Bradley, D. P. Rogers, J. B. Edson, and G. S. Young, 1996: Bulk parameterization of air–sea fluxes for Tropical Ocean Global Atmosphere Coupled Ocean–Atmosphere Response Experiment. *J. Geophys. Res.,* **101,** 3747–3764.

Garratt, J. R., 1977: Review of drag coefficients over oceans and continents. *Mon. Wea. Rev.,* **105,** 915–929.

Gaynor, J. E., and C. F. Ropelewski, 1979: Analysis of the convectively modified GATE boundary layer using in situ and acoustic sounder data. *Mon. Wea. Rev.,* **107,** 985–993.

Houze, R. A., Jr., 1989: Observed structure of mesoscale convective systems and implications for large-scale heating. *Quart. J. Roy. Meteor. Soc.,* **115,** 425–461.

Jabouille, P., J.-L. Redelsperger, and J.-P. Lafore, 1994: Modification of surface fluxes by atmospheric convection. *Proc. Sixth Conf. on Mesoscale Processes,* Portland, OR, Amer. Meteor. Soc., 9–12.

Jorgensen, D. P., T. J. Matejka, and M. A. LeMone, 1995: Structure and momentum fluxes within a TOGA/COARE squall line system observed by airborne doppler radar. *Proc. 21st Conf. on Hurricanes and Tropical Meteorology,* Miami, FL, Amer. Meteor. Soc., 579–581.

LeMone, M. A., 1980: The marine boundary layer. *Workshop on the Planetary Boundary,* Boston, MA, Amer. Meteor. Soc.

——, and W. T. Pennell, 1976: The relationship of trade wind cumulus distribution to subcloud layer fluxes and structure. *Mon. Wea. Rev.,* **104,** 524–539.

——, D. P. Jorgensen, S. Lewis, B. Smull, and T. Matejka, 1995: Boundary layer recovery in the stratiform region of mesoscale convective systems in TOGA COARE. *Proc. 21st Conf. on Hurricanes and Tropical Meteorology,* Miami, FL, Amer. Meteor. Soc., 509–511.

Lin, X., 1995: Diurnal variations of convection over the western pacific warm pool region during the TOGA COARE IOP. *Proc. 21st Conf. on Hurricanes and Tropical Meteorology,* Miami, FL, Amer. Meteor. Soc., 91–93.

Lin, Y.-L., R. D. Farley, and H. D. Orville, 1983: Bulk parameterization of the snow field in a cloud model. *J. Climate Appl. Meteor.,* **22,** 1065–1092.

Liu, W. T., K. B. Katsaros, and J. A. Businger, 1979: Bulk parameterization of the air–sea exchange of heat and water vapor including the molecular constraints at the interface. *J. Atmos. Sci.,* **36,** 1722–1735.

Malkus, J. S., 1958: On the structure of the trade wind moist layer. *Physical Oceanography and Meteorology,* Massachusetts Institute of Technology and Woods Hole Oceanographic Institute Monogr., No. 2, 47 pp.

——, 1962: Ideas and observations on progress in the study of the seas. *Physical Oceanography,* Vol. 1, *The Sea,* M. N. Hill, Ed., John Wiley and Sons, 88–294.

Parsons, D., and Coauthors, 1994: The integrated sounding system: Description and preliminary observations from TOGA COARE. *Bull. Amer. Meteor. Soc.,* **75,** 553–567.

Roll, H. U., 1965: *Physics of the Marine Atmosphere.* Academic Press, 426 pp.

Rotunno, R., and K. A. Emanuel, 1987: An air–sea interaction theory for tropical cyclones. Part II: Evolutionary study using a nonhydrostatic axisymmetric numerical model. *J. Atmos. Sci.,* **44,** 542–561.

——, J. B. Klemp, and M. L. Weisman, 1988: A theory for strong, long-lived squall lines. *J. Atmos. Sci.,* **45,** 463–485.

Rutledge, S. A., and P. V. Hobbs, 1984: The mesoscale and microscale structure and organization of clouds and precipitation in midlatitude clouds. Part II: A diagnostic modeling study of precipitation development in narrow cold frontal rainbands. *J. Atmos. Sci.,* **41,** 2949–2972.

Smolarkiewicz, P. K., 1983: A simple positive definite advection scheme with small implicit diffusion. *Mon. Wea. Rev.,* **111,** 479–486.

——, 1984: A fully multidimensional positive definite advection transport algorithm with small implicit diffusion. *J. Comput. Phys.,* **54,** 325–362.

——, and W. W. Grabowski, 1990: The multidimensional positive advection transport algorithm: Nonoscillatory option. *J. Comput. Phys.,* **86,** 355–375.

Simpson, J., and W.-K. Tao, 1993: The Goddard Cumulus Ensemble Model. Part II: Applications for studying cloud precipitating processes and for NASA TRMM. *Terr. Atmos. Oceanic Sci.,* **4,** 73–116.

Tao, W.-K., and J. Simpson, 1993: The Goddard Cumulus Ensemble Model. Part I: Model description. *Terr. Atmos. Oceanic Sci.,* **4,** 35–72.

——, ——, and S.-T. Soong, 1991: Numerical simulation of a subtropical squall line over Taiwan Strait. *Mon. Wea. Rev.,* **119,** 2699–2723.

——, ——, C.-H. Sui, B. Ferrier, S. Lang, J. Scala, M.-D. Chou, and K. Pickering, 1993: Heating, moisture and water budgets of tropical and midlatitude squall lines: Comparisons and sensitivity to longwave radiation. *J. Atmos. Sci.,* **50,** 673–690.

Trier, S. B., W. C. Skamarock, M. A. LeMone, D. B. Parsons, and D. P. Jorgensen, 1996: Structure and evolution of the 22 February 1993 TOGA COARE squall line: Numerical simulations. *J. Atmos. Sci.,* **53,** 2861–2886.

Webster, P. J., and R. Lukas, 1992: TOGA COARE: The Coupled Ocean–Atmosphere Response Experiment. *Bull. Amer. Meteor. Soc.,* **73,** 1377–1416.

Young, G. S., D. V. Ledvina, and C. W. Fairall, 1992: Influence of precipitating convection on the surface energy budget observed during a tropical ocean global atmosphere pilot cruise in the tropical western Pacific Ocean. *J. Geophys. Res.,* **97,** 9595–9603.

——, S. M. Perugini, and C. W. Fairall, 1995: Convective wakes in the equatorial western pacific during TOGA. *Mon. Wea. Rev.,* **123,** 110–123.

Zhang, D.-L., and R. A. Anthes, 1982: A high-resolution model of the planetary boundary layer—Sensitivity tests and comparisons with SESAME-79 data. *J. Appl. Meteor.,* **21,** 1594–1609.

Zipser, E. J., 1977: Mesoscale and convective-scale downdrafts as distinct components of squall line structure. *Mon. Wea. Rev.,* **105,** 1568–1589.